



HAL
open science

Structural and electrical properties of $\text{BaTi}_{1-x}\text{ZrxO}_3$ sputtered thin films: effect of the sputtering conditions

Vincent Reymond, Sandrine Payan, Dominique Michau, Jean-Pierre Manaud, Mario Maglione

► To cite this version:

Vincent Reymond, Sandrine Payan, Dominique Michau, Jean-Pierre Manaud, Mario Maglione. Structural and electrical properties of $\text{BaTi}_{1-x}\text{ZrxO}_3$ sputtered thin films: effect of the sputtering conditions. *Thin Solid Films*, 2004, 467 (1-2), pp.54-58. 10.1016/j.tsf.2004.03.005 . hal-00159589

HAL Id: hal-00159589

<https://hal.science/hal-00159589v1>

Submitted on 1 Dec 2023

HAL is a multi-disciplinary open access archive for the deposit and dissemination of scientific research documents, whether they are published or not. The documents may come from teaching and research institutions in France or abroad, or from public or private research centers.

L'archive ouverte pluridisciplinaire **HAL**, est destinée au dépôt et à la diffusion de documents scientifiques de niveau recherche, publiés ou non, émanant des établissements d'enseignement et de recherche français ou étrangers, des laboratoires publics ou privés.

Structural and electrical properties of $\text{BaTi}_{1-x}\text{Zr}_x\text{O}_3$ sputtered thin films: effect of the sputtering conditions

Reymond Vincent^a, Payan Sandrine^a, Michau Dominique^a, Manaud Jean-Pierre^a, Maglione Mario^a

^a Univ. Bordeaux, CNRS, Bordeaux INP, ICMCB, UMR 5026, F-33600 Pessac, France

Abstract : $\text{BaTi}_{1-x}\text{Zr}_x\text{O}_3$ thin films have been prepared on Si and Pt/TiO₂/SiO₂/Si substrates by radio-frequency magnetron sputtering varying the deposition parameters, such as the chamber pressure, the substrate temperature and the gas composition. The films have been probed by X-ray Diffraction (XRD), Wavelength Dispersive Spectrometry (WDS), Scanning Electron Microscopy (SEM) and Rutherford Backscattering Spectrometry (RBS). The dependence of their composition, crystallinity and dielectric properties on these parameters was investigated. The films show dielectric susceptibilities up to 130, dielectric losses of 2% and tunabilities up to 17% under 650 kV/cm at 100 kHz.

Keywords : Thin films ; $\text{BaTi}_{1-x}\text{Zr}_x\text{O}_3$ sputtering ; Dielectric properties ; Structural properties

1. Introduction

The processing of dynamic random access memory (DRAM) and other integrated capacitor structures requires thin films materials with a high dielectric constant and low leakage current. Barium strontium titanate (BST), with cubic perovskite structure, has been considered as a promising material for such application [1,2], because of its high dielectric permittivity at room temperature. However, although the BST composition has been optimized, the dielectric losses are still high and its breakdown field is rather low for the production of electronic devices. In addition, for agile high frequency filters and lines, the tunability of BST is not always compatible with the low losses requirements.

New materials are then desirable to meet all these requirements. Similarly to BST, the Curie temperature of BaTiO_3 is shifted below room temperature by the addition

of zirconium. The dielectric properties thus depend on the zirconium content and have been extensively studied for the bulk ceramic: the solid solution $\text{BaTiO}_3\text{-BaZrO}_3$ shows the highest dielectric susceptibility at room temperature for a 25% Zr substitution in the crystal structure. Therefore, $\text{BaTi}_{1-x}\text{Zr}_x\text{O}_3$ (BTZ) with $x > 0.25$ is a paraelectric material at room temperature with a high dielectric constant and low dielectric dispersion against frequency. Moreover, for the compositions between 26% and 40%, bulk ceramics display a relaxor behaviour [3]. The same desirable properties are expected for new designs, as thin films.

Several deposition routes are conceivable to obtain homogeneous, crack-free and crystallized films of BTZ. Spin-on coating of sol-gel solution [4], MOCVD [5,6] and hydrothermal method [7] were recently shown to be suitable for BTZ films, but required high-reactive precursors; physical vapor deposition technique has been successfully used for BST films [8,9] and low Zr-content BTZ films ($x < 0.3$) [10–12]. Our BTZ films with $0.25 < x < 0.6$ have been then deposited by radio-frequency magnetron sputtering. In order to characterize the BTZ films as a function of the experimental parameters, the films were prepared with various chamber pressures, substrate temperatures and re-

* Corresponding author. Tel.: +33-5-40-00-26-97; fax: +33-5-40-00-27-61.

E-mail address: reymond@icmcb.u-bordeaux.fr (V. Reymond).

active gas compositions. X-ray diffraction (XRD), Wavelength Dispersive Spectrometry (WDS), Rutherford Backscattering Spectrometry (RBS), Scanning Electron Microscopy (SEM) and electrical measurements have been used to study the influence of the deposition parameters on the films composition, crystallinity, and dielectric properties. $\text{Ba}_{0.6}\text{Sr}_{0.4}\text{TiO}_3$ thin films were also deposited in the same conditions as a reference.

2. Experimental details

2.1. Preparation of BTZ thin films

The target was a cold-pressed and sintered $\text{BaTi}_{1-x}\text{Zr}_x\text{O}_3$ ceramic: BaCO_3 , ZrO_2 and TiO_2 powders were first mixed, ball milled and calcinated at 1200°C during 15 h; a 50-mm diameter target was then pressed into disk and sintered for 4 h at 1400°C under oxygen atmosphere. The composition of the ceramic target was optimized in order to give the BTZ films the chosen stoichiometry.

The films were prepared by radio-frequency magnetron sputtering on $\text{Pt/TiO}_2/\text{SiO}_2/\text{Si}$ (150 nm of Pt) and silicon commercial wafers with (111) and (100) respective orientations. The substrate was first rinsed with acetone, put in an ultrasonic bath of demineralized water and cleaned by condensation of propanol vapor at its surface.

It was then placed in the sputtering chamber parallel to the target, at a distance of 55 mm, and heated at a temperature in the range of $500\text{--}700^\circ\text{C}$. The sputtering chamber was first pumped down to a pressure of 6×10^{-5} Pa. A dioxygen/pure argon plasma (0 to 20% of O_2) was used as sputtering gas at a total pressure of 0.5 to 7 Pa. An rf power of 2.6 W/cm^2 was chosen and the BTZ target was presputtered for 1 h to stabilize the surface composition. The film thicknesses were optimized for the forthcoming characterizations: depending on the deposition time and conditions, the films thicknesses ranged from 115 to 170 nm (1 h) on Si substrates for the structural characterizations, and from 500 to 700 nm (3.5 h) on $\text{Pt/TiO}_2/\text{SiO}_2/\text{Si}$ substrates for the dielectric experiments. The detailed sputtering conditions of the BTZ thin films are summarized in Table 1. BST thin films were deposited in the same conditions from a $\text{Ba}_{0.6}\text{Sr}_{0.4}\text{TiO}_3$ target.

Table 1
Sputtering conditions for BTZ film preparation

Target material	Cold-pressed $\text{BaTi}_{1-x}\text{Zr}_x\text{O}_3$ ($x=0.15$ to 0.35), 50 mm diameter
Target-substrate distance	55 mm
Initial pressure of chamber	6×10^{-5} Pa
Substrate temperature	500 to 700°C
Sputtering time	1 and 3.5 h
Sputtering gas	Ar– O_2 mixture (0 to 20% O_2)
Sputtering pressure	0.5 to 7 Pa
rf power	2.6 W cm^{-2}

2.2. Characterization of BTZ thin films

The crystal structure of the as-deposited thin films was probed by XRD using Cu $\text{K}\alpha$ radiation. WDS (SX-50, CaMeCa, 10 kV) and RBS (NEC, 2 MeV, $^4\text{He}^+$, 5° of incident angle) were used to analyse the stoichiometry of the films. Their thickness was determined from contact profilometry, SEM side views (JEOL 840, 15 kV) WDS and RBS data.

The electrical measurements were conducted on the film by making a metal/insulator/metal capacitor. The top electrodes were prepared at room temperature using rf magnetron sputtering: the films were first etched through a mask under argon (0.5 Pa) during 5 min at 0.15 W/cm^2 in order to clean the surface, and platinum electrodes, 150 nm in thickness, were deposited through this mask (with 12 $500\text{-}\mu\text{m}$ diameter holes). Their exact area was determined using optical microscopy. The dielectric properties of each capacitor were investigated by observing the frequency (f) and the electric field (E) dependence of the permittivity ϵ' and dissipation factor $\tan \delta$, using an impedance-gain phase analyser (Hewlett Packard 4194A). The frequency and voltage ranged respectively from 100 Hz to 15 MHz and from -40 to $+40$ V. The tunability, corresponding to the decrease of ϵ' with the applied field E , is expressed as $T=[\epsilon'(E)-\epsilon'(E=0)]/\epsilon'(E=0)$.

3. Results and discussion

3.1. Film structure and composition

Fig. 1 shows the effect of the total sputtering pressure on XRD patterns of BTZ films. Perovskite peaks are observed under given conditions. A higher pressure allows a better crystallinity of the films: highly polycrystalline films were obtained above 3 Pa, whereas lower pressures only give amorphous films. This evolution is in good agreement with the one observed by Im et al. [9] in BST thin films, which we confirm for our BST films. The same improvement of the crystallinity is moreover observed by increasing the substrate temperature and by decreasing the oxygen percentage in the gas mixture. Crystallized films with non-textured structure are then obtained for a certain range of parameters, without any post-annealing treatment being necessary. The insetted graph in Fig. 1 shows the (110) peaks for the target and a film. The observed shift of all the films' peaks to the low angle side as compared to the target corresponds to an excess of Zr in the films (x close to 0.35 instead of 0.20 in the target). The same behaviour is observed among bulk ceramics when increasing the Zr content. This increase of the lattice constant can also be due to internal stresses, that are often observed in thin films [13].

Fig. 2 shows a SEM cross-sectional micrograph of a film. The films are dense and have a smooth surface. The picture shows three layers, which allows the determination

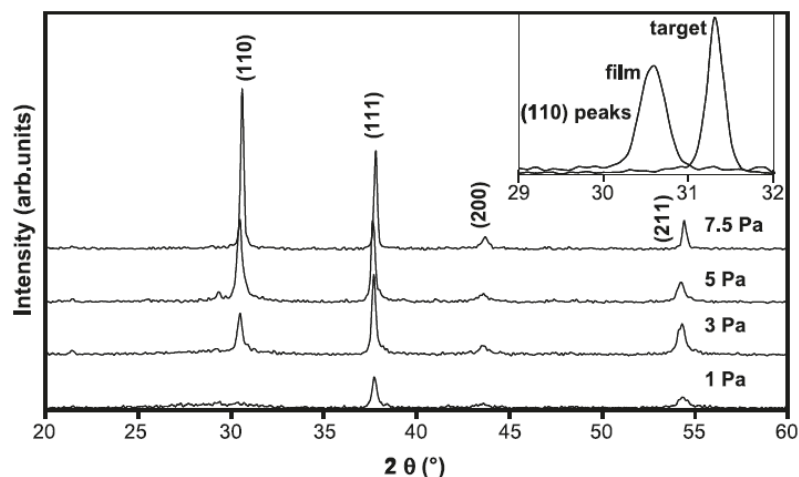


Fig. 1. Evolution of the BTZ thin films crystallinity with the sputtering pressure. XRD patterns of BTZ films, deposited from a $\text{BaTi}_{0.80}\text{Zr}_{0.20}\text{O}_3$ target at 600°C and 1% O_2 . Inset: shift of the film (111) peak compared to the target peak.

of the film thickness: the upper one is the BTZ layer (615 nm) while the both lower belong to the substrate (210 nm of Pt/TiO₂).

The composition of the films was investigated using RBS. The Pt bottom layer prevents the chemical analysis on Pt/TiO₂/SiO₂/Si substrate, because the energy peaks of zirconium overlap with those of platinum. Films on silicon were then probed after deposition in the same conditions as those on platinized substrates. WDS analysis of samples on both substrates was performed to check the film composition and to compute the thicknesses, which agreed with the already measured one from contact profilometry and SEM pictures (Fig. 2). Fig. 3 shows typical RBS data of a BTZ film on Si substrate. Two curves are superimposed: the experimental one and a simulation using the software RUMP (Computer Graphics Service). The channels for barium, zirconium and titanium are well separated owing to the weak thickness of the film (1 h of sputtering). This allows the determination of the site A/site B ratio for the ABO₃ perovskite structure and then the composition of the depos-

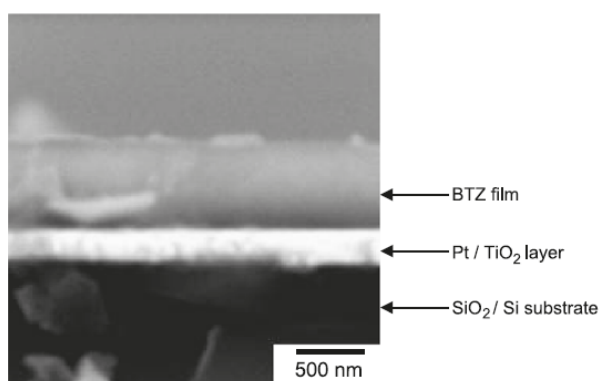


Fig. 2. SEM micrograph of a BTZ film deposited on Pt/TiO₂/SiO₂/Si substrate at 650°C under 5 Pa, 1% O_2 .

ited layer. The cationic ratios Ba/(Ti+Zr) ranged from 0.55 to 0.95 for a $\text{BaTi}_{0.65}\text{Zr}_{0.35}\text{O}_3$ target depending on the sputtering conditions (giving films with barium contents lower than 1 and zirconium contents between 0.5 and 0.6). The stoichiometry of the ceramic target is not retained during the growth of the films by rf magnetron sputtering. The relatively high deposition velocity (2.5 nm/min) and the sputtering yield of each species prevent having the same Ba/(Ti+Zr) ratio in the target and the films: WDS and RBS analyses indicate that the Zr content in the thin films is always greater than in the target material. For a given target composition, this difference can be tuned—but not cancelled—on changing the sputtering parameters. This is consistent with the lines shift in XRD analysis. The target composition may also be fitted to obtain the chosen film stoichiometry.

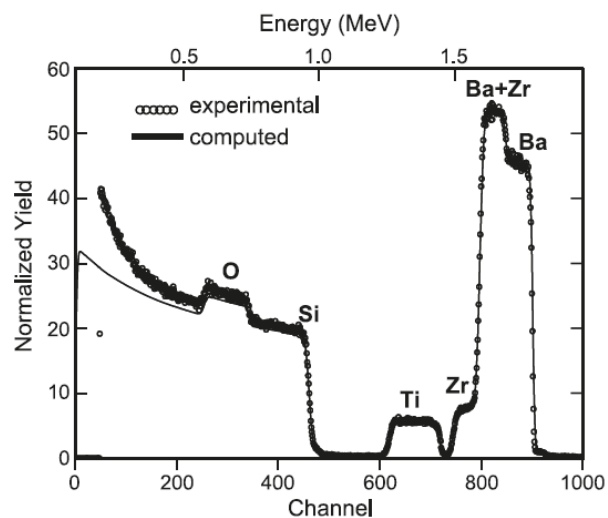


Fig. 3. RBS data and its simulation of a $\text{Ba}_{0.94}\text{Ti}_{0.70}\text{Zr}_{0.30}\text{O}_3$ film deposited on Si substrate at 600°C under 5 Pa, 1% O_2 .

3.2. Dielectric properties

Fig. 4 shows the tunability–electric field ($T-E$) characteristic of BTZ films ($x=0.30$) in a Pt/BTZ/Pt capacitor configuration, deposited at various chamber pressures. The dielectric permittivity of the films at zero field ranges from 30 to 130, with a strong dependence on the deposition pressure. Their tunability also depends on the pressure, with a maximum value of 17% at 650 kV/cm for a pressure of 5 Pa. Beyond this pressure, no improvement of the dielectric parameters was observed. In the same way, at 5 Pa, a deterioration of the tunability at 650 kV/cm down to 3% is observed by decreasing the substrate temperature from 650 to 500 °C. The tunability is also divided by 3 by increasing the O₂ partial pressure in the gas mixture from 1% to 20%. The evolution of these properties is thus closely linked to the crystallinity of the films (Fig. 1).

Furthermore, the pressure and oxygen content impact could be explained by defects and distortions in the structure that would appear at low total sputtering pressures and high oxygen partial pressure. In fact, a high deposition rate associated to a low total pressure could lead to high density of defects, which is consistent with XRD. The impact of the dioxygen is more difficult to evaluate because an increase of the O₂ content leads, on the one hand, to a decrease of the deposition rate, but on the other hand, to a modification of the resputtering of the film during its growth.

The evolution of the permittivity and tunability (at 800 kV/cm) as a function of the Ba/(Ti+Zr) ratio is shown on Fig. 5. These characteristics were measured for each capacitor at 100 kHz. The best properties were finally obtained for the following sputtering conditions: 5 Pa, 650 °C and 1%O₂ from a Ba-rich target leading to films with a cationic ratio close to one and 30% of Zr in B site. The dielectric losses also depend on this ratio but no obvious trend is deduced from our data. For all the films, they were always between 1% and 3%. First rapid thermal annealing treatments (at 600

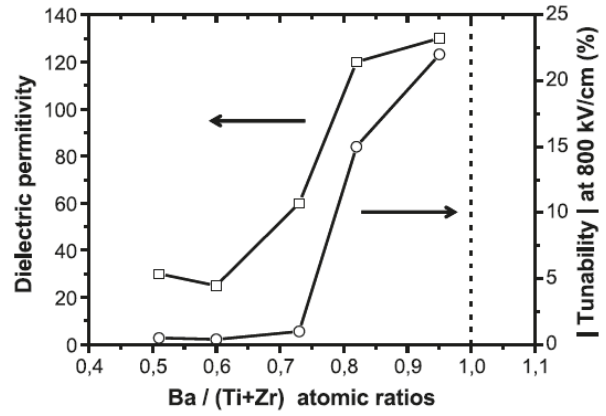


Fig. 5. Permittivity and tunability dependencies on the Ba/(Ti+Zr) ratio of BTZ films deposited from targets of different compositions (between 15% and 35% of Zr).

°C under air, after films deposition) allowed to reduce the losses by a factor 2, without modification of the other dielectric characteristics. This reduction of the losses is attributed to an improvement of the top Pt electrode/BTZ interface.

From this point of view, our BTZ films do not display improved dielectric properties as compared to similar BST films, even if the evolutions of their crystallinity, stoichiometry and dielectric properties with the deposition parameters are consistent with the observations on our BST films.

The temperature dependence of the dielectric properties of BTZ films was recently probed between 150 and 350 K for our BTZ films. The dielectric constant exhibited no real maximum, confirming previous results on sputtered films [10,11]. Moreover, no dielectric dispersion was observed at any temperature. However, recent reports by Jiwei et al. [14] and Dixit et al. [15] on sol–gel deposited BTZ films showed a frequency dependence for a broad maximum of the dielectric constant. We thus conclude that the processing

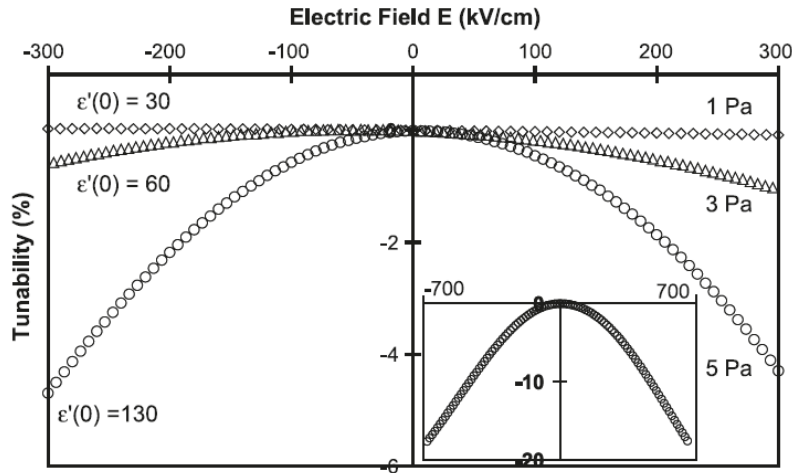


Fig. 4. Influence of the sputtering total pressure on the tunability of BTZ thin films ($x=0.30$) deposited at 650 °C, 1% O₂. Inset: Tunability (up to 650 kV/cm) of the film deposited at 5 Pa.

route (either sputtering or sol–gel) is a key parameter for the films to be relaxor or not.

4. Conclusion

BTZ thin films were successfully deposited by rf magnetron sputtering on Si and Pt/TiO₂/SiO₂/Si substrates. Perovskite phase was formed, adjusting the experimental deposition parameters. Polycrystalline thin films were then obtained, with various cationic ratios. The chamber pressure, oxygen partial pressure and substrate temperature were found to play a crucial role in the films structure and composition. The dielectric properties are closely linked to both characteristics. Atomic Force Microscopy investigations are currently in progress in order to determine the impact of the sputtering parameters on the films surface morphologies that may also influence the dielectric properties.

A dielectric constant of 130 at 100 kHz combined with a tunability of 17% at 650 kV/cm was obtained on a 600-nm highly polycrystalline Ba_{0.95}Ti_{0.7}Zr_{0.3}O₃ thin film, deposited on a Pt/TiO₂/SiO₂/Si substrate heated at 650 °C under a 5 Pa total pressure, 1%O₂ rich. Optimized sputtering conditions thus allow the improvement of crystallinity, stoichiometry and dielectric properties. Interesting dielectric properties were already reported in low-Zr content BTZ films ($x=0.12$) by Wu [10]. To our knowledge, this is the first time that a such tunability is observed for Zr-rich BTZ thin films.

Even if BTZ films do not display improved dielectric properties as compared to similar BST films, their relatively low dielectric constant and potential relaxor behaviour are attractive for microwave frequency applications, the processing route (either sputtering or sol–gel) being a key parameter for the films to be relaxor or not.

Acknowledgements

This work was supported by the Conseil Régional d'Aquitaine and The European Union through FEDER funds. The authors are grateful to P. Moretto and L. Serani for their help in RBS measurements.

References

- [1] A. Kozyrev, V. Keis, V. Osadchy, A. Pavlov, O. Buslov, L. Sengupta, *Integr. Ferroelectr.* 34 (2001) 189.
- [2] J. Serraiocco, B. Acikel, P. Hansen, T. Taylor, H. Xu, J.S. Speck, R.A. York, *Integr. Ferroelectr.* 49 (2002) 161.
- [3] J. Ravez, A. Simon, *Eur. J. Solid State Inorg. Chem.* 34 (1997) 1199.
- [4] A. Dixit, S.B. Majumder, A. Savvinov, R.S. Katiyar, R. Guo, A.S. Bhalla, *Mater. Lett.* 56 (2002) 933.
- [5] T. Tohma, H. Masumoto, T. Goto, *Jpn. J. Appl. Phys., Part 1* 41 (11B) (2002) 6643.
- [6] R. Pantou, C. Dubourdieu, F. Weiss, J. Kreisel, G. Köbemik, W. Haessler, *Mater. Sci. Semicond. Process.* 5 (2003) 237.
- [7] T. Kawano, K. Hashimoto, A. Nishida, T. Tsuchiya, *J. Ceram. Soc. Jpn.* 110 (6) (2002) 530.
- [8] S. Yamamichi, H. Yabuta, T. Sakuma, Y. Miyasaka, *Appl. Phys. Lett.* 64 (13) (1994) 1644.
- [9] J. Im, O. Auciello, P.K. Baumann, S.K. Streiffer, *Appl. Phys. Lett.* 76 (5) (2000) 627.
- [10] T.-B. Wu, C.-M. Wu, M.-L. Chen, *Thin Solid Films* 334 (1998) 77.
- [11] W.S. Choi, B.S. Jang, Y. Roh, J. Yi, B. Hong, *J. Non-Cryst. Solids* 303 (2002) 190.
- [12] M.-C. Wang, C.-Y. Chen, C.-S. Hsi, N.-C. Wu, *J. Cryst. Growth* 246 (2002) 99.
- [13] S.B. Desu, *Phys. Stat. Solidi, A* 141 (1994) 119.
- [14] Z. Jiwei, Y. Xi, Z. Liangying, S. Bo, H. Chen, *J. Cryst. Growth* 262 (2004) 341.
- [15] A. Dixit, S.B. Majumder, R.S. Katiyar, A.S. Bhalla, *Appl. Phys. Lett.* 82 (6) (2003) 2679.